Task ID: 425.018
Task Title: Destruction of Perfluoroalkyl Surfactants in Semiconductor Process Waters Using Boron Doped Diamond Film Electrodes
Deliverable: Report on the susceptibility of a variety of PFAS compounds to electrolysis at BDD anodes and cathodes

Summary Abstract:

Perfluoroalkyl sulfonate (PFAS) compounds are widely used in semiconductor manufacturing. The most commonly used PFAS compound in the electronics industry is perfluorooctyl sulfonate (PFOS). Studies conducted in the late 1990s have shown that PFOS bioaccummulates in humans, fish and other animals (1). The American Red Cross reported a mean PFOS serum level of 34.9 μg/L in donated blood, and mean serum levels in other countries have been found to range from 17 to 53 μg/L (2). PFOS does not break down in the environment and has an elimination half-life of 4 years in the human body (2).

Because of PFOS accumulation in the environment, the United State Environmental Protection Agency (EPA) and several European governments have proposed banning the use of PFOS (3). Most replacements for PFOS are shorter chain length PFAS compounds, with perfluorobutane sulfonate (PFBS) being the most widely used. Although PFBS has smaller bioconcentration factors than PFOS, it still accumulates in the environment and is nonbiodegradable.

This research investigated oxidation of perfluroalkyl sulfonate (PFAS) including perfluorooctane sulfonate (PFOS) and perfluorobutane sulfonate (PFBS) using anodes composed of boron-doped diamond (BDD) films on p-silicon substrates. Experiments measuring oxidation rates of PFOS and PFBS were performed at different current densities and temperatures using a rotating disk electrode (RDE) reactor and a parallel plate flow-through reactor. Both PFOS and PFBS oxidation produced carbon dioxide, sulfate, fluoride, and trace amounts of trifluoracetic acid (TFA). TFA accounted for less than 3% of the PFOS or PFBS removed from the solutions. Reaction rates in the RDE reactor were zeroth order in concentration, which is indicative of a reaction limited by the availability of reactive sites. Reaction rates in the flow-through reactor were first order in concentration due to mass transfer limitations. Apparent activation energies for PFOS and PFBS were consistent with an unactivated process, which were determined by measuring the reaction rates in the RDE as a function of temperature. Density functional simulations were used to calculate the reaction energies and activation barriers for both PFOS and PFBS oxidation by two different mechanisms: oxidation by hydroxyl radicals and direct electron transfer. High activation barriers (i.e. PFBS: 123 ~ 288 kJ/mol; PFOS: 122 ~ 241 kJ/mol) for $HO^{\bullet}$ attack at different sites on the PFAS molecule indicated that oxidation by hydroxyl radicals was not the rate limiting mechanism for PFAS oxidation. Activation energies for direct electron transfer calculated as a function of the electrode potential indicated that the experiments were performed at sufficiently high overpotentials, which allowed the reactions to proceed via an activationless direct electron transfer mechanism.

Technical Results and Data:

Figure 1 shows PFOS concentrations as a function of electrolysis time for current densities ranging from 1 to 20 mA/cm^2 at a temperature of 22 °C. Reaction rates were zeroth order in PFOS concentration over the entire range of current densities. This behavior is indicative of reactive site saturation at the electrode surface. Faradaic current efficiencies, defined as the fraction of the cell current going towards PFOS oxidation, declined with increasing current density. Assuming complete oxidation requires 34 electrons per PFOS molecule (4 per carbon atom and 2 for sulfur), the Faradaic current efficiencies ranged from 100% at a current density of 1 mA/cm^2 to 20% at a current density of 20 mA/cm^2.

The detectable reaction products consisted of sulfate, fluoride, and trace levels of trifluoroacetic acid (TFA). Over the course of the experiments, the measured solution pH values decreased from 4 to ~2.3**,** which is indicative of carbonic acid production. The trace amounts of TFA recovered represented less than 3% of the PFOS removed. One sulfate and an average of 11±0.5 fluoride ions were produced per PFOS oxidized. The recovery of only 11 out of 17 fluoride ions per PFOS removed indicates that there were losses of volatile compounds from the solution. These volatile compounds likely include TFA, HOF and possibly HF. Loss of hypofluorite (HOF) from the solution was qualitatively indicated by the presence of a bleach-like odor.

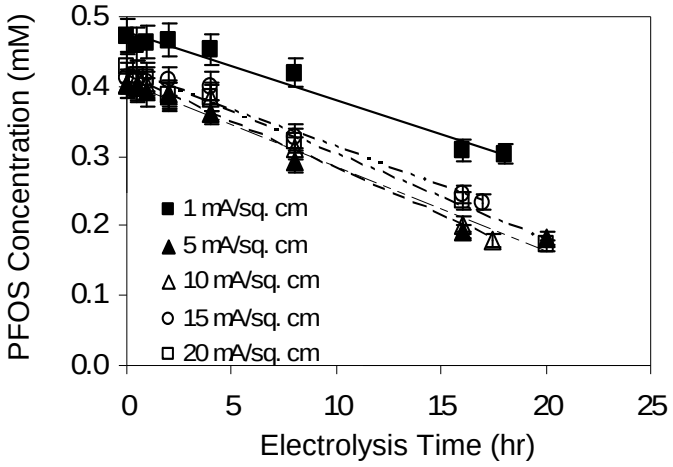

Figure 1. PFOS concentrations in the RDE reactor as a function of electrolysis time at current densities ranging from 1 to 20 mA/cm^2 at 22 °C.

To prevent the loss of volatile compounds, experiments were performed in a gas-tight, flow-through reactor. Figure 2 shows the decline in PFOS and TOC concentrations as a function of the electrolysis time at a current density of 20 mA/cm^2 and 22 °C. PFOS reaction rates in the flow-through reactor were first order in concentration. The difference in reaction order between the flow-through and RDE experiments can be attributed to mass transfer limitations in the flow-through reactor. For example, the zeroth order rate constant measured using the RDE at a current density of 20 mA/cm^2 would result in complete PFOS removal after only 8 minutes.

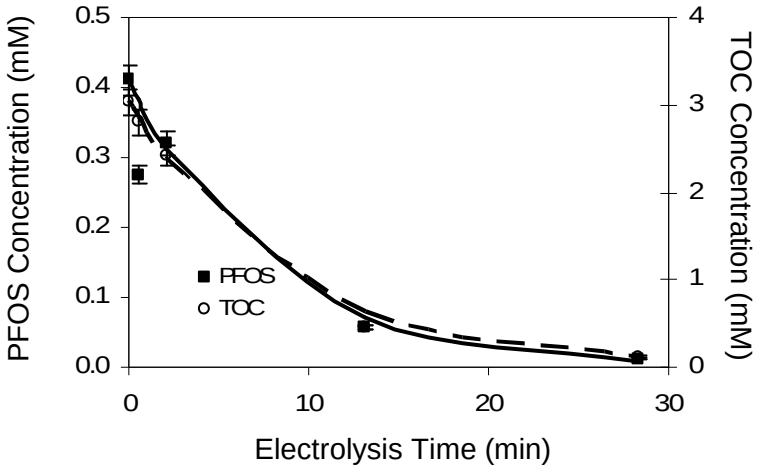

Figure 2. PFOS and TOC concentrations as a function of electrolysis time in the flow-through reactor operated at a current density of 20 mA/cm^2 at 22 °C.

The reaction products in the flow-through system were the same as those in the RDE reactor except for a greater fluoride mass balance. The fluoride mass balance increased to 14 out of 17 in the flow-through reactor. Only trace levels of TFA, representing less than 3% of the PFOS removed, were detected.

PFBS oxidation at BDD anode is similar to that of PFOS oxidation. As seen in figure 3 the reaction rates were also zeroth order in PFBS concentration over the entire range of current densities in the RDE reactor. In the flow-through reactor the reaction rate was first order at lower concentrations. The major products include sulfate and fluoride ions. The only organic reaction product detected was trifluoroacetic acid (TFA), which appeared at trace levels representing <3% of the PFBS removed.

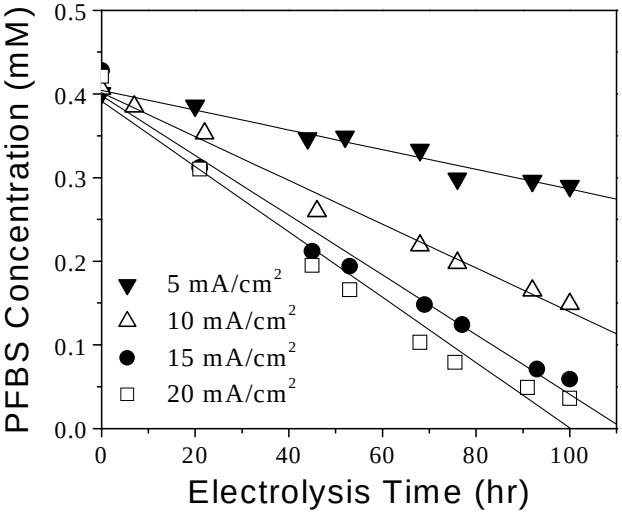

Figure 3. PFBS concentration as a function of electrolysis time at current density of 5, 10, 15 and 20 mA/cm^2 in an RDE reactor.

The temperature dependence of the PFAS reaction rates can be used to help determine the rate-limiting step for the reaction mechanism. PFBS reaction rates measured at 7, 15, 22, 25 and 45 °C were used to determine the apparent activation

energies for PFBS oxidation, as illustrated in the Arrhenius plot shown in Figure 4. The data in Figure 4 yield an apparent activation energy of 9.3 ± 3 kJ/mol. Reactions with activation barriers this low generally proceed readily at room temperature (4). Similar experiments at a fixed electrode potential yielded an apparent activation energy of 4.2 kJ/mol for PFOS oxidation.

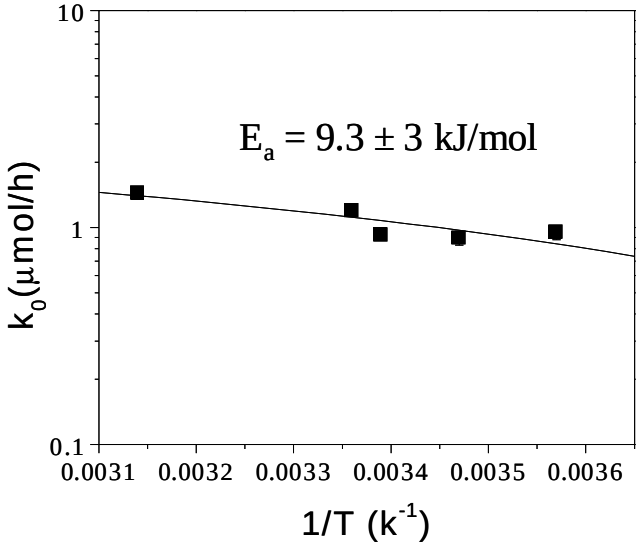

Figure 4. Arrhenius plot of zeroth order rate constants for PFBS oxidation at a fixed current density of 10 mA/cm^2.

DFT simulations were performed to determine the activation barriers for the reaction of hydroxyl radicals at different sites on the PFAS molecule. Figure 5 shows the transition state and final product for hydroxyl radical attack at the $-SO_3^-$ group for a PFBS molecule. The reaction produced HSO_4^- and a nonafluoro-1-butane radical with an overall reaction energy of -84 kJ/mol. The activation energy determined from the transition state was 123 kJ/mol. Hydroxyl radical activation barriers this high are generally associated with reactions that do not readily occur at room temperature (4). For example, activation energies for $HO^\bullet$ reaction with perchlorinated biphenyls (PCBs) range from 71 to 93 kJ/mol (5, 6). This is consistent with the lack of PCB oxidation by hydroxyl radicals at room temperature. In contrast, phenol, which readily reacts with hydroxyl radicals, has activation barriers ranging from 4 to 25 kJ/mol, depending on the site of attack (7).

DFT simulations were used to determine the activation energies for direct oxidation of PFBS as a function of the electrode potential using the methods described in Anderson and Kang (8). DFT simulations indicate that loss of one electron leads to lengthening of the C-S bond, and that the C-S bond length closely approximates the reaction coordinate (*i.e.*, >90% of the energy change between the reactant and the transition state is due to C-S bond lengthening). Figure 6a shows the energy of the reactant (PFBS anion) and products (PFBS neutral radical + electron) as a function of the C-S bond length at a potential of 2.5 V/SHE. Product energies as a function of electrode potential were determined by shifting the energy profile of the product species downwards by 106.1 kJ (*i.e.*, 1.0 eV) to increase the electrode potential by 1.0 V and upwards by 106.1 kJ to decrease the electrode potential by 1.0 V (8). Energies from the vacuum scale were

converted to the SHE scale by subtracting 4.6 eV (8). The higher the electrode potential, the shorter the C-S bond stretching required for the reactant and product energy profiles to intersect. Intersection of the two energy profiles yields the bond length at the transition state and the activation energy for the reaction:

$$C_4F_9SO_3^- \rightarrow C_4F_9SO_3^{\bullet} + e^- \qquad (1)$$

By shifting the products energy profile up and down, activation energies as a function of electrode potential were calculated, as shown in Figure 6b. Figure 6b shows that the activation energy decreases from 270 kJ/mol at a potential of 1.0 V/SHE to zero at a potential of 3.0 V/SHE. This indicates that the reaction becomes activationless at potentials greater than 3.0 V/SHE, and is consistent with the low apparent activation energy calculated in Figure 4.

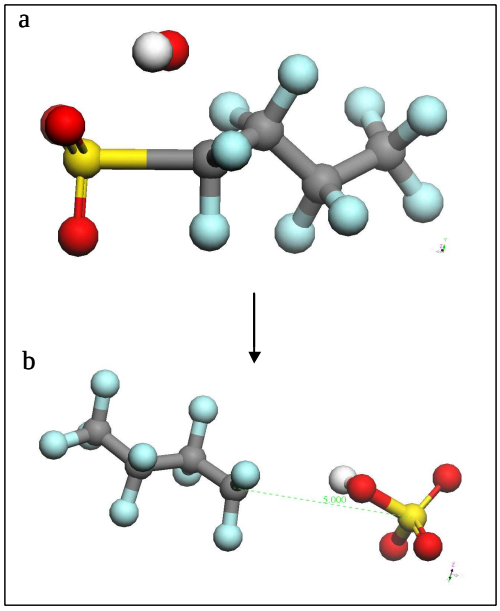

Figure 5. Transition state (a) and final products (b) for hydroxyl radical attack at the $-SO_3^-$ group for a PFBS molecule.

Density functional theory (DFT) simulations were also performed on PFOS. DFT simulations found that the activation energies for hydroxyl radical oxidation of PFOS at different reaction sites ranged from 122 to 241 kJ/mol. These high activation barriers are consistent with the lack of reactivity of PFOS with conventional hydrogen peroxide base advanced oxidation processes. DFT calculated activation barriers for direct oxidation of PFOS indicated that the reaction is activationless at electrode potentials higher than 2.7 V with respect to the standard hydrogen electrode (SHE). The low experimentally measured activation barrier and the calculated activationless electron transfer reaction at potentials above 2.7 V/SHE indicates that direct electron transfer is the rate limiting step for PFOS oxidation.

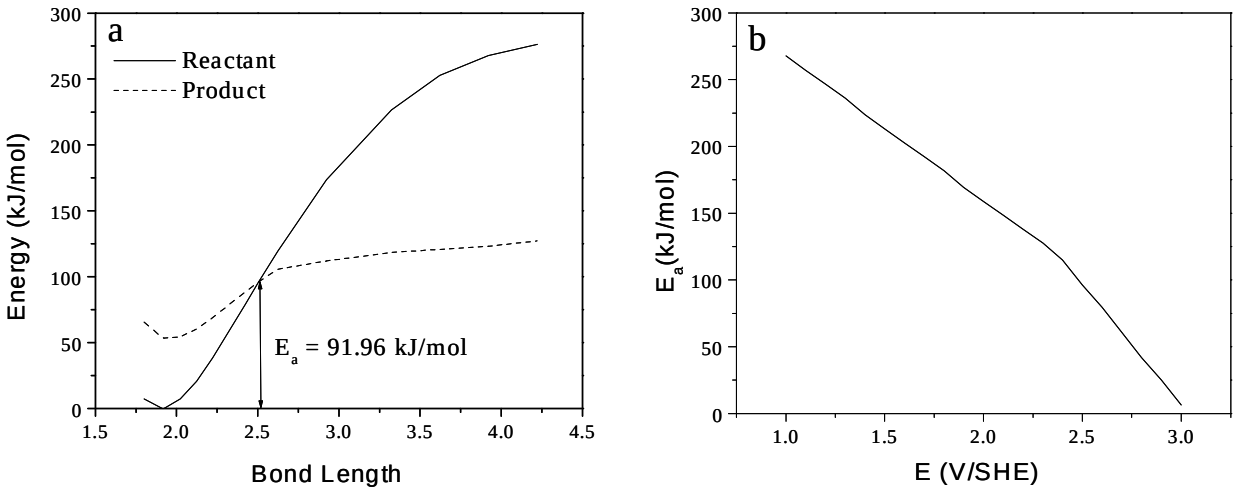

Figure 6. a) Energy profiles for reactant ($C_4F_9SO_3^-$) and products ($C_4F_9SO_3^{\bullet} + e^-$) for vertical electron transfer as a function of the C-S bond length at an electrode potential of 2.5 V/SHE. b) Activation energies as a function of electrode potential for a direct electron transfer reaction.

References

(*1*) Giesy, J. P.; Kannan, K. Global Distribution of Perfluorooctane Sulfonate in Wildlife. *Environ. Sci. Technol.* **2001**, 35, 1339-1342.
(*2*) Organization for Economic Co-operation and Development. Hazard assessment of perfluorooctane sulfonate (PFOS) and its salts. ENV/JM/RD (2002)17/FINAL, November 21, 2002.
http://www.fluorideaction.org/pesticides/pfos.final.report.nov.2002.pdf
(*3*) Environmental Protection Agency. Federal Register, 67, 326. Dec. 9, 2002. *Perfluoroalkyl Sulfonates*: *Significant New Use*
(*4*) Wade, L.G. Jr. *Organic Chemistry*, Prentice Hall, 4th edition, 1999.
(*5*) Murena, F. Schioppa, E.; Gioia, F., *Environ. Sci. Technol*. **2000**, 34, 4382-4385.
(*6*) Lin, Y. J.; Chen, Y. L.; Huang, C. Y.; Wu, M. F., *J. Hazard. Mater.* **2006**, 136, 902-910.
(*7*) Wang, Y.; Liu, Y.; Luo, Y.; Zhang, W.; Zhong, R.; *Acta Phys.-Chim. Sin*. 2006, 22, 1266-1271.
(*8*) Anderson, A. F.; Kang, D. B. *J. Phys. Chem. A*, **1998**, 102, 5993-5996.